RSC Advances

PAPER

View Article Online
View Journal | View Issue

Cite this: *RSC Adv.*, 2025, **15**, 49301

Mechanism of methanol steam reforming with inverse ZrO_2/Cu catalyst

Jie Feng,†[a] Tingting Zhang,†[c] Guozhi Zhao,[b] Chengxiang Li,[b] Xuan Wu,[b] Jiaqiang Sun,[b] Yu Wang,*[d] Kun Liu*[e] and Guofeng Zhao*[ab]

Received 19th September 2025
Accepted 1st December 2025

DOI: 10.1039/d5ra07097j

rsc.li/rsc-advances

The highly active inverse ZrO_2/Cu catalyst used in methanol steam reforming reaction was confirmed by XRD and HRTEM. Control experiments and characterization results consistently differentiated surface and interfacial hydroxyl groups. For the catalyst enriched in interfacial OH, the reaction preferentially proceeded through the formate pathway. However, for the catalyst enriched in surface OH, methyl formate pathway preferentially existed on its surface. This work reveals the role of OH plays in the methanol steam reforming reaction, preliminarily establishing foundation for the investigation of H_2O-participated reactions.

1 Introduction

Hydrogen energy, as a clean and renewable energy source, plays a crucial role in resolving the global energy crisis and mitigating environmental challenges. However, its widespread application is currently restrained by issues such as storage safety risks, high transportation costs, and the difficulty of hydrogen production.[1,2] In contrast, methanol, with a high hydrogen content of up to 12.5 wt% and relatively safe transport properties, has emerged as a promising carrier for hydrogen storage and transportation.[3–7] The hydrogen stored in methanol can be efficiently released *via* the methanol steam reforming (MSR) reaction (eqn (1)). Nevertheless, side reaction occurring during the MSR process (eqn (2)) decreases hydrogen impurity, which significantly hinders its practical utilization. Therefore, the development of high efficient MSR catalyst and the comprehensive understanding of the MSR mechanism is of great importance.[1,8,9]

$$CH_3OH + H_2O \xrightarrow{200-350\ ^\circ C} CO_2 + 3H_2 \quad (1)$$

$$CH_3OH \xrightarrow{200-400\ ^\circ C} CO + 2H_2 \quad (2)$$

MSR reaction is a complex, multi-step process including the steps such as methanol dehydrogenation, hydroxyl dissociation, and the water–gas shift reaction.[10] The reaction mechanism is commonly proposed to proceed *via* three primary pathways: (1) methanol undergoes dehydrogenation to form formaldehyde, which subsequently decomposes into carbon monoxide and hydrogen; carbon monoxide then reacts with water through the water–gas shift reaction, yielding carbon dioxide and hydrogen.[11] (2) Methanol dehydrogenates to generate methoxy species, which react with methanol to produce methyl formate; methyl formate subsequently decomposes into formate species, which further decompose into carbon dioxide and hydrogen.[12] (3) Methanol dehydrogenates to form formaldehyde, which is oxidized by water to form formic acid; formic acid then decomposes into carbon dioxide and hydrogen.[13] Hence, a comprehensive investigation of the reaction mechanism, particularly the structure–function relationships of active sites, is essential for enhancing the efficiency and selectivity of the reaction.[14] Such insights also provide a scientific basis for the rational design of catalysts, facilitating industrial-scale applications.

In our previous work, we have developed an effective inverse ZrO_2/Cu (ZrO_2: ~2–3 nm, Cu: ~10–15 nm) for the MSR reaction.[15] The work mainly investigated the adsorption and desorption of the intermediates such as HCHO, $HCOOCH_3$. Additionally, traditional Cu/ZrO_2 or inverse ZrO_2/Cu have also been reported in the MSR reaction by other groups and the effects (such as the pivotal intermediate HCOO–Cu,[16] Cu size,[17] Cu valence,[17] and ZrO_2 crystal phase[18]) have been investigated. However, the role of hydroxyl species playing in MSR reaction is still unclear. Moreover, the hydroxyl species plays an important

[a]*Shanghai Key Laboratory of Green Chemistry and Chemical Processes, School of Chemistry and Molecular Engineering, East China Normal University, Shanghai 200062, China. E-mail: gfzhao@ahnu.edu.cn*

[b]*Anhui Basic Discipline Research Center for Clean Energy and Catalysis, College of Chemistry and Materials Science, Anhui Normal University, Wuhu 241002, China*

[c]*School of Foreign Languages, Shandong First Medical University & Shandong Academy of Medical Sciences, Taian 271016, China*

[d]*Frontiers Science Center for Transformative Molecules, Zhangjiang Insititute for Advanced Study, Shanghai Jiao Tong University, Shanghai 200240, China. E-mail: wangyusjtu@sjtu.edu.cn*

[e]*Institute of Optical Functional Materials for Biomedical Imaging, School of Chemistry and Pharmaceutical Engineering, Shandong First Medical University & Shandong Academy of Medical Sciences, Taian 271016, China. E-mail: liukun2436@126.com*

† The authors contribute equally to this work.

role in H_2O-related reactions, such as MSR reaction,[19] water gas shift reaction,[20] and CO preferential oxidation reactions.[21] This work reveals that on the ZrO_2/Cu catalyst, the surface OH (on ZrO_2 surface) and interfacial OH (at ZrO_2–Cu interface) coexist, the interfacial OH being more active in the MSR reaction. *In situ* diffuse reflectance infrared fourier-transform spectroscopy (*in situ* DRIFTS) confirmed that methanol adsorbed on surfaces rich in interfacial hydroxyl groups undergoes the formate pathway,[22] leading to the formation of CO_2 and H_2 (CH_3OH + interfacial OH → CH_3O*, CH_3O* + interfacial OH → HCOOH → CO_2 + H_2O). In contrast, on surfaces with surface hydroxyl groups, which react with methanol to produce *COOH. Subsequently, *COOH reacts with CH_3OH to form methyl formate. Finally, methyl formate decomposes to CH_3O* (CH_3O* transform to formate to accomplish to catalytic cycle) (CH_3OH + surface OH → *COOH, *COOH + CH_3OH → $HCOOCH_3$ → CH_3O*, CH_3O* + minor interfacial OH → HCOOH → CO_2 + H_2O). This reaction mechanism highlights the critical role of hydroxyl groups in determining catalytic performance, establishing the foundation of developing high performance MSR catalysts.

2 Experimental

The detailed catalyst preparation, catalyst characterization, and catalyst evaluation (Fig. S1) were exhibited in the SI. Note that: fresh ZrO_2-0.25/Cu (weight content of ZrO_2 was 25%) without other pre-treatment condition, the sample was abbreviated as ZrO_2-0.25/Cu-dried. For the fresh ZrO_2-0.25/Cu under (H_2O-bubbling atmosphere H_2O bubbling in He flow (30 mL min^{-1}) for 30 min), the sample was labelled as ZrO_2-0.25/Cu-humidified. For the fresh ZrO_2-0.25/Cu after reduced (H_2/He mixed gas (5 vol% H_2)) for 30 min, (300 °C), the sample was named as ZrO_2-0.25/Cu-reduced.

3 Results and discussion

3.1 Structures and chemical states of catalysts

In our previous work, we found that ZrO_2-0.1/Cu exhibited excellent catalytic performance in MSR reaction (~60% methanol conversion and 100% CO_2 selectivity at 250 °C).[15] However, for this catalyst, we found that the OH species couldn't be detected by *in situ* DRIFTS. Hence, ZrO_2-0.25/Cu (the weight content of ZrO_2 was 0.25) was selected to investigate the role of OH species playing in this reaction (ZrO_2-0.25/Cu exhibited ~60% methanol conversion and 100% CO_2 selectivity at 250 °C, Fig. S2). XRD pattern (Fig. 1A) revealed that only characteristic diffraction peaks of CuO phase were detected, with the most prominent peak intensity observed for the (111) crystal plane. Notably, no characteristic diffraction peaks of ZrO_2 were identified. Subsequent quantitative analysis of ZrO_2 loading through ICP-OES (Table S1) demonstrated that ZrO_2 loading of 22.01 wt% in the ZrO_2-0.25/Cu catalyst. This finding aligns with the absence of ZrO_2 crystalline phase detection in XRD patterns, indicating that ZrO_2 exists in a highly dispersed state on the CuO surface,[23] which is consistent with our previous studies.[15] To investigate the surface morphology of the catalyst, transmission electron microscopy (TEM) analysis was performed (Fig. 1B). Distinct lattice fringes with spacings of 0.254 nm and 0.294 nm were clearly observed on the ZrO_2-0.25/Cu surface, corresponding to the (111) plane of CuO and the (011) plane of tetragonal ZrO_2 (t-ZrO_2), respectively.[24] This observation further confirms the uniform dispersion of fine ~3–4 nm t-ZrO_2 particles on the ~10–15 nm CuO substrate in the ZrO_2-0.25/Cu catalyst, rather than the absence of t-ZrO_2 components.[25] Moreover, for the reduced catalyst, XRD and TEM techniques (Fig. 1A and C) indicated that the ZrO_2/CuO composite transforms to ZrO_2/Cu (ZrO_2, 3–4 nm, Cu 15–20 nm; ZrO_2 and Cu particle size derived from Scherrer equation are 3.5 and 16 nm, respectively), which may play an important role in the MSR reaction. The well-defined lattice structures and interfacial characteristics align with previous reports on Cu/ZrO_2 heterojunction systems, where such structural configurations enhance catalytic performance through synergistic effects.

3.2 Distinguish surface OH from interfacial OH

Derived from previous works, OH plays an important role in the H_2O-related reactions,[26] but the surface and interfacial OH hasn't been investigated. From these previous works, we know that H_2-reduction or H_2O (D_2O)-bubbling are two vital roles to introduce OH (OD) into the catalyst. So, ZrO_2-0.25/Cu-dried, ZrO_2-0.25/Cu-humidified, and ZrO_2-0.25/Cu-reduced were tentatively investigated by H_2O-TPD to investigate the surface and interfacial OH (Fig. 2). H_2O-TPD profiles reveal two characteristic desorption regions: peak at 180–200 °C corresponding to active interfacial hydroxyl groups (at ZrO_2/Cu interface), and those near 340 °C representing weakly active surface hydroxyl species (on ZrO_2 surface).[27] Notably, the ZrO_2-0.25/Cu-dried exhibited a minor concentration of hydroxyl groups, probably contributing to its negligible catalytic activity (~1% methanol conversion at 250 °C). Meanwhile, the ZrO_2-0.25/Cu-humidified shows substantially quantities of surface hydroxyl groups, likely corresponding with its inferior catalytic activity (~5% methanol conversion at 250 °C). Remarkably and interestingly, for ZrO_2-0.25/Cu-reduced, apart from the surface hydroxyl groups at 340 °C, the prominent H_2O-desorption peak at 180–200 °C appeared, tentatively attributed to interfacial OH and corresponding with its excellent catalytic activity (~60% methanol conversion at 250 °C).

Subsequently, CH_3OH-adsorbed ZrO_2-0.25/Cu-dried, ZrO_2-0.25/Cu-humidified, and ZrO_2-0.25/Cu-reduced at different temperatures were investigated by *in situ* DRIFTS to differentiate surface from interfacial OH (Fig. 3). The absorption bands at 3650–3550 cm^{-1} are attributed to isolated hydroxyl groups on the zirconia surface, those at 3700–3650 cm^{-1} correspond to surface hydroxyl groups on zirconia,[28] and those at 3750–3700 cm^{-1} are associated with interfacial hydroxyl groups between zirconia and copper, predominantly in the form of Zr–(OH)–Cu.[29] For ZrO_2-0.25/Cu-dried, the interfacial hydroxyl group content is nearly absent (Fig. 2). At 175 °C, as methanol enters the reaction, the hydroxyl groups undergo transformations. Upon methanol introduction, methanol undergoes decomposition on the zirconia surface, generating methoxy and

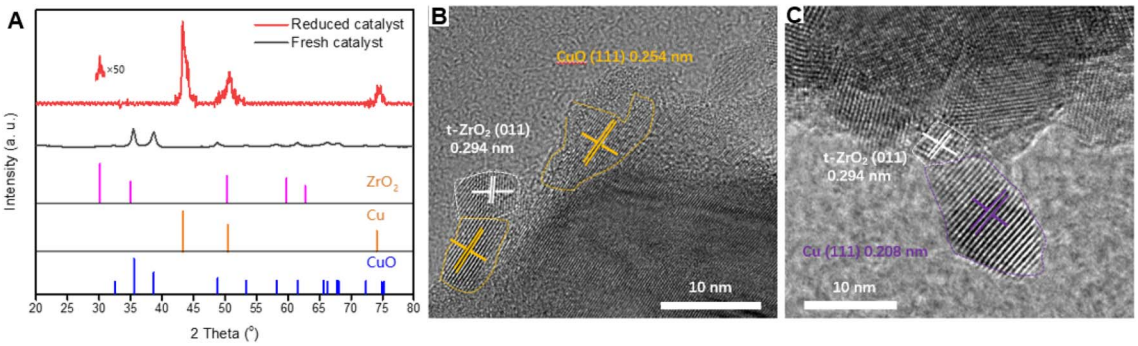

Fig. 1 (A) XRD patterns of fresh ZrO_2-0.25/Cu and ZrO_2-0.25/Cu-reduced; (B) HRTEM image of fresh ZrO_2-0.25/Cu; (C) HRTEM image of ZrO_2-0.25/Cu-reduced.

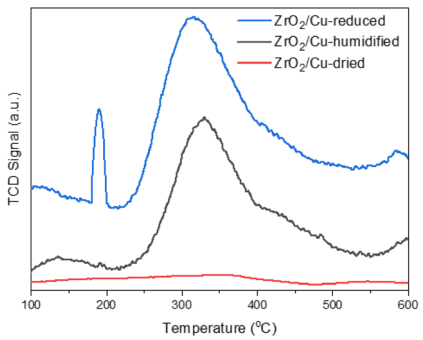

Fig. 2 H_2O-TPD profiles of ZrO_2/Cu-reduced, ZrO_2/Cu-humidified, and ZrO_2/Cu-dried.

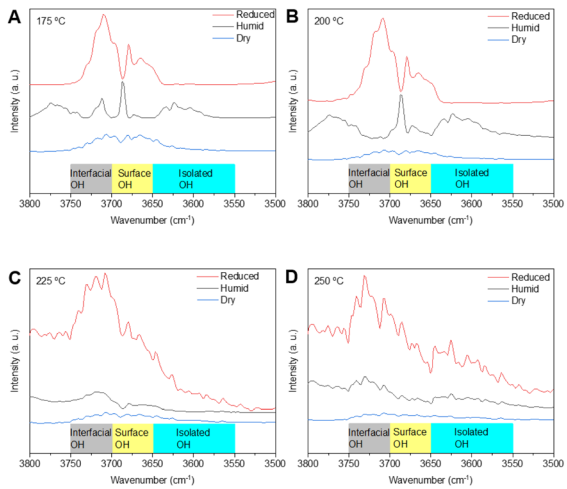

Fig. 3 Amplified *in situ* DRIFTS (3800–3500 cm^{-1}, to differentiate surface OH from interfacial OH) of ZrO_2/Cu-reduced, ZrO_2/Cu-humidified, and ZrO_2/Cu-dried after methanol reaction for 3 min at different temperatures ((A) 175 °C, (B) 200 °C, (C) 225 °C, (D) 250 °C).

hydrogen species. The hydrogen (from OH of CH_3OH) preferentially reacts with surface oxygen to form surface hydroxyl groups (Fig. 3). The minimal amount of carbon dioxide detected (corresponding to the C=O stretching vibration at 2360 cm^{-1}) indicates low activity of these surface hydroxyl groups (Fig. 4). In contrast, for ZrO_2-0.25/Cu-humidified, due to the presence of water, it exhibits a substantial amount of surface hydroxyl groups with minor interfacial hydroxyl groups (Fig. 3), corresponding with its moderate CO_2 production (Fig. 4). For ZrO_2-0.25/Cu-reduced, the catalyst surface contains a significant amount of interfacial hydroxyl groups (Fig. 3), leading to an unusually high CO_2 yield (Fig. 4). Notably, with the increasing of temperature (175–250 °C), surface OH transforms to interfacial OH, forming the active Zr–(OH)–Cu structure (can be observed for ZrO_2-0.25/Cu-humidified and obviously found for ZrO_2-0.25/Cu-reduced). Hence, the interfacial OH plays an important role in MSR reaction and a part of surface OH could transforms to interfacial OH.

3.3 Reaction mechanism

In the MSR reaction, H_2O can dissociate at the surface or the interface site to form OH species.[30] For ZrO_2-0.25/Cu-dried, with the increase of temperature from 175 °C to 250 °C, the C=O stretching vibrations of methyl formate (Fig. 5, at 1740 and

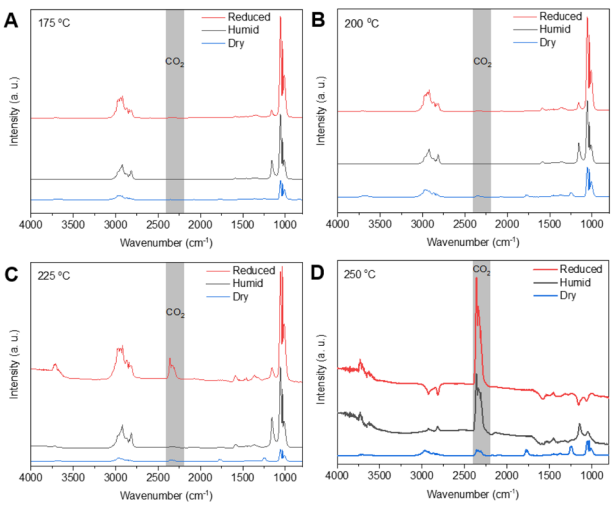

Fig. 4 Amplified *in situ* DRIFTS (4000–900 cm^{-1}, to differentiate CO_2) of ZrO_2/Cu-reduced, ZrO_2/Cu-humidified, and ZrO_2/Cu-dried after methanol reaction for 3 min at different temperatures ((A) 175 °C, (B) 200 °C, (C) 225 °C, (D) 250 °C).

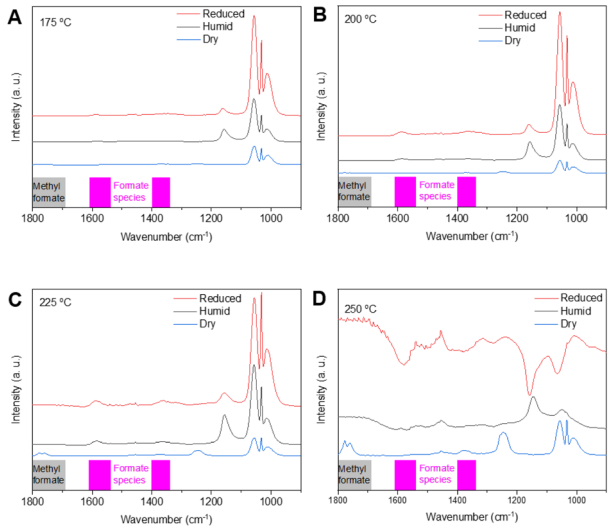

Fig. 5 Amplified *in situ* DRIFTS (1800–900 cm^{-1}, to differentiate methyl formate from formate species) of ZrO_2/Cu-reduced, ZrO_2/Cu-humidified, and ZrO_2/Cu-dried after methanol reaction for 3 min at different temperatures ((A) 175 °C, (B) 200 °C, (C) 225 °C, (D) 250 °C).

1780 cm^{-1}) increase progressively.[23] Meanwhile, no significant change attributed to surface OH is observed in the peak region at 3700–3650 cm^{-1} (Fig. 3), and the peak at 2360 cm^{-1} assigned as CO_2 (Fig. 4) is considerably lower compared to the other two samples. These observations consistently suggest that in the absence of interfacial hydroxyl groups, the reaction preferentially proceeds *via* the methyl formate pathway (Fig. 6A), resulting in low catalytic activity. For ZrO_2-0.25/Cu-humidified and ZrO_2-0.25/Cu-reduced, interfacial hydroxyl groups coexist on the catalyst surface. However, ZrO_2-0.25/Cu-reduced exhibits a higher interfacial hydroxyl content. With the increase of temperature from 175 to 250 °C, formate species (at 1580 and 1380 cm^{-1}, corresponding to the asymmetric and symmetric COO) is appeared (Fig. 5), with the intensity of ZrO_2-0.25/Cu-reduced being higher.[31] Meanwhile, CO_2 content displays a relatively higher content (Fig. 4). These findings indicate that, in the presence of interfacial hydroxyl groups, the reaction proceeds through the formate pathway (Fig. 6B), leading to significantly enhanced catalytic activity. For ZrO_2-0.25/Cu-dried, with the increase of temperature from 175 °C to 250 °C, the C=O stretching vibrations of methyl formate (Fig. 5, at 1740 and 1780 cm^{-1}) increase progressively.[20] Meanwhile, no significant change attributed to surface OH is observed in the peak region at 3700–3650 cm^{-1} (Fig. 3), and the peak at 2360 cm^{-1} assigned as CO_2 (Fig. 4) is considerably lower compared to the other two samples. These observations consistently suggest that in the absence of interfacial hydroxyl groups, the reaction proceeds *via* the methyl formate pathway (Fig. 6A), resulting in low catalytic activity. For ZrO_2-0.25/Cu-humidified and ZrO_2-0.25/Cu-reduced, interfacial hydroxyl groups coexist on the catalyst surface. However, ZrO_2-0.25/Cu-reduced exhibits a higher interfacial hydroxyl content. With the increase of temperature from 175 to 250 °C, formate species (at 1580 and

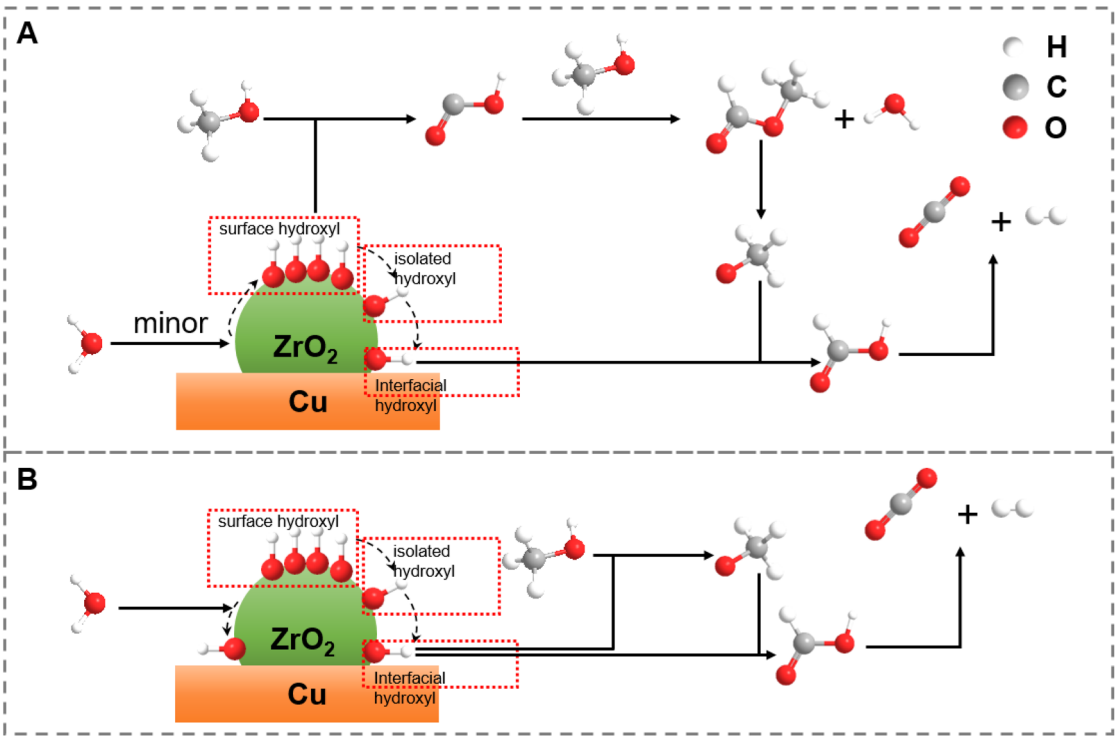

Fig. 6 Reaction mechanism of MSR reaction on ZrO_2/Cu. (A) Catalyzed by surface OH through methyl formate pathway; CH_3OH + surface OH → *COOH, *COOH + CH_3OH → $HCOOCH_3$ → CH_3O*, CH_3O* + minor interfacial OH → HCOOH → CO_2 + H_2O (B) catalyzed by interfacial OH *via* formate species pathway; CH_3OH + interfacial OH → CH_3O*, CH_3O* + interfacial OH → HCOOH → CO_2 + H_2O.

1380 cm^{-1}, corresponding to the asymmetric and symmetric COO) is appeared (Fig. 5), with the intensity of ZrO_2-0.25/Cu-reduced being higher.[27] Meanwhile, CO_2 content displays a relatively higher content (Fig. 4). These findings indicate that, in the presence of interfacial hydroxyl groups, the reaction preferentially proceeds through the formate pathway (Fig. 6B), leading to significantly enhanced catalytic activity.

3.4 Discussion

Moreover, in order to further corroborate the pivotal role of interfacial OH playing in MSR reaction, the control experiments were designed. From the H_2O-TPD experiment, we know that the peaks at ~200 and ~300–400 °C are attributed to the removal of interfacial and surface OH (Fig. 2). Hence, we treated the ZrO_2/Cu-reduced under pure He flow at 180 °C to partly remove the interfacial OH. Form Fig. S4, with the treatment time from 1 to 5 min, the peaks (at ~200 °C) corresponding to interfacial OH decease suddenly and the ones corresponding to surface OH (at 300–400 °C) are nearly unchanged. Meanwhile, the He-treated ZrO_2/Cu-reduced (He: 1, 5 min) could also catalyze methanol steam reforming reaction at 180 °C just using the residual interfacial OH (200 mg catalyst, N_2 flow of 30 mL min^{-1}, and methanol of 1 g h^{-1}). The initial methanol conversions using the ZrO_2/Cu-reduced, ZrO_2/Cu-reduced-He-1 min (ZrO_2/Cu-reduced treated under He flow for 1 min at 180 °C), and ZrO_2/Cu-reduced-He-5 min (ZrO_2/Cu-reduced treated under He flow for 5 min at 180 °C) catalyst were 7%, 2%, 1%, respectively, corresponding well with the H_2O-TPD spectra. Hence, the control experiment further testifies the pivotal role of interfacial OH other than surface OH playing in this reaction.

Up to date, most endeavors are focused on Cu-based catalysts, especially Cu–ZrO_2, because of their attractive low-temperature MSR activity and its substantial potential against CO formation.[15] For example, Ritzkopf *et al.*[32] prepared a nano-Cu/ZrO_2 catalyst by the micro-emulsion method, achieving a lower CO selectivity of below 0.1 vol% at 300 °C with a hydrogen productivity comparable to the commercial Cu/ZnO catalyst. Indeed, in the whole process, for our inverse ZrO_2/Cu and Cu/ZrO_2,[32] catalysts, the CO selectivity is very low. Thus, we confidently believe that the Cu–ZrO_2 interface is beneficial to the formation of CO_2 other than CO (both inverse ZrO_2/Cu and traditional Cu/ZrO_2 interface) at low temperature (<300 °C). From the H_2O-TPD results (Fig. S5), we could see that for the traditional Cu/ZrO_2,[32] the content of interfacial OH is similar to that of our inverse ZrO_2/Cu, so, our inverse ZrO_2/Cu exhibits similar activity (250 °C, 60% methanol conversion and 99.9% CO_2 selectivity) compared with that of traditional Cu/ZrO_2 (250 °C, 58% methanol conversion and 99.9% CO_2 selectivity[32]).

4 Conclusion

Through H_2O-TPD and *in situ* DRIFTS analyses, we identified that MSR reaction preferentially proceeds through the formate pathway on the highly active ZrO_2-0.25/Cu-reduced catalyst enriched with interfacial hydroxyl groups. However, for ZrO_2-0.25/Cu-dried, methyl formate pathway preferentially exists on its surface, due to the existence of surface hydroxyl groups (absence of interfacial hydroxyl groups). These findings provide a novel perspective for the design of metal–oxide model catalysts, offering valuable insights to accelerate the industrial application of such systems.

Conflicts of interest

The authors declare that there is no conflicts of interest.

Data availability

The data that support the findings of this study are available on request from the corresponding author. The data are not publicly available due to privacy or ethical restrictions.

Supplementary information (SI): the details of catalyst preparation, catalyst characterization, catalyst evaluation, IR flowchart, and H_2O-TPD. See DOI: https://doi.org/10.1039/d5ra07097j.

Acknowledgements

This work was funded by the National Natural Science Foundation of China (grant no. 22179038), the high score discipline construction project of Anhui Province (project no. 061920), and the Young People Fund of Shandong first medical university (202201-037).

References

1 M. Xiao, Y. Zhang, X. Wang and L. Liu, *Angew. Chem., Int. Ed.*, 2024, **63**, e202407640.
2 M. Zabilskiy, X. Huang, J. Zheng and K. M. Neyman, *Angew. Chem., Int. Ed.*, 2021, **60**, 4912–4920.
3 K. Yu, W. Tong and S. Tsang, *Nat. Commun.*, 2012, **3**, 1230.
4 L. Lin, W. Zhou and D. Ma, *Nature*, 2017, **544**, 80–83.
5 C. Rameshan, W. Stadlmayr and C. B. Klötzer, *Angew. Chem., Int. Ed.*, 2010, **49**, 3224–3227.
6 X. He, Y. Wang and H. Liu, *ACS Catal.*, 2019, **9**, 2213–2221.
7 J. Shen and C. Song, *Catal. Today*, 2002, **77**, 89–98.
8 M. Kusche, A. Friedrich, T. Braun and J. J. Weigand, *Angew. Chem., Int. Ed.*, 2013, **52**, 5022–5025.
9 F. Ji, Y. Li, C. Zhou and W. Wang, *Energy Sci. Eng.*, 2019, **7**, 1200–1208.
10 A. Hassan, *Int. J. Hydrogen Energy*, 2024, **93**, 1487–1501.
11 M. A. Achomo, P. Muthukumar and N. R. Peela, *Int. J. Hydrogen Energy*, 2025, **140**, 1111–1125.
12 J. L. C. Fajín, M. Natália and D. S. Cordeiro, *ACS Catal.*, 2022, **12**, 512–526.
13 K. Ma, Y. Tian and Z. Zhao, *Chem. Sci.*, 2019, **10**, 2578–2584.
14 X. Zhang, M. Zhang and Y. Deng, *Nature*, 2021, **589**, 396–401.
15 X. Xu, T. Lan and G. Zhao, *Appl. Catal., B*, 2023, **334**, 122839–122851.
16 C. Wu, L. Lin, J. Liu, J. Zhang, F. Zhang, T. Zhou, N. Rui, S. Yao, Y. Deng, F. Yang, W. Xu, J. Luo, Y. Zhao, B. Yan, X. Wen, J. Rodriguez and D. Ma, *Nat. Commun.*, 2020, **11**, 5767.

17 M. Song, W. Zeng, L. Li, X. Wu, G. Li and C. Hu, *Ind. Eng. Chem. Res.*, 2023, **62**, 3898–3908.
18 M. Song, L. Li, X. Wu, H. Cai, G. Li and C. Hu, *Catalysts*, 2024, **14**, 480.
19 R. Thattarathody and M. Artoul, *Ind. Eng. Chem. Res.*, 2018, **57**, 3175–3186.
20 X. Sun, J. Yu and Y. Han, *Nat. Chem.*, 2024, **16**, 2044–2053.
21 I. Sadykov, D. Palagin and F. Krumeich, *J. Catal.*, 2024, **429**, 115363–115374.
22 P. Luo, P. Shi and C. Li, *Appl. Catal., A*, 2025, **689**, 120006–120025.
23 H. Zhao, R. Yu and S. Ma, *Nat. Catal.*, 2022, **5**, 818–831.
24 X. Chen, Z. Feng and D. Zhao, *Catal. Sci. Technol.*, 2022, **12**, 7048–7056.
25 X. Li, Q. Liu and H. Wu, *Chem*, 2022, **8**, 2148–2162.
26 L. Luo, J. Luo and H. Li, *ACS Catal.*, 2022, **12**, 11272–11280.
27 Y. Hu, Z. Liang and Y. Zhang, *EES Catal.*, 2024, **2**, 365–378.
28 V. F. Kispersky, Y. Chen and S. P. Crossley, *J. Phys. Chem. C*, 2014, **118**, 16424–16433.
29 H. D. Zhu, S. Wang and S. Wang, *Int. J. Hydrogen Energy*, 2025, **109**, 1452–1460.
30 D. Li, R. Qiu, B. Moskowitz, Z. Jiang, H. Gu, Q. Wen, I. Wachs and M. Zhu, *J. Am. Chem. Soc.*, 2025, **147**, 24040–24049.
31 C. Wu, L. Lin and J. Liu, *Nat. Commun.*, 2020, **11**, 5767–5776.
32 I. Ritzkopf, S. Vukojevic, C. Weidenthaler, J. Grunwaldt and F. Schuth, *Appl. Catal., A*, 2006, **302**, 215–223.